Archives of Materials Science and Engineering

Volume 114
Issue 1
March 2022
Pages 34-41

International Scientific Journal
published monthly by the
World Academy of Materials
and Manufacturing Engineering

DOI: 10.5604/01.3001.0015.9851

Prediction of brittle fracture propagation behaviour of hydroxyapatite (HAp) coating in artificial femoral stem component

C.H. Sheng [a], M. Nagentrau [b,*], N.H. Ibrahim [b]

[a] School of Engineering, UOW Malaysia KDU University College, Shah Alam, Selangor, Malaysia
[b] School of Computer Science and Engineering, Faculty of Innovation and Technology, Taylor's University, Taylor's Lakeside Campus, Subang Jaya, Selangor, Malaysia
* Corresponding e-mail address: nagentrau.rau17@yahoo.com
ORCID identifier: https://orcid.org/0000-0002-0736-3467 (M.N.)

ABSTRACT

Purpose: This study addresses the brittle fracture propagation behaviour modelling of hydroxyapatite (HAp) coating in artificial femoral stem component.

Design/methodology/approach: A simple two dimensional flat-on-flat contact configuration finite element model consisting contact pad (bone), Ti-6Al-4V substrate and HAp coating is employed in static simulation. The HAp coating is modelled as elastic layer with pre-microcrack which assumed to be initiated due to stress singularity.

Findings: The study revealed that reducing coating thickness, pre-microcrack length and artificial femoral stem elastic modulus along with increasing bone elastic modulus will result in significant stress intensity factor (SIF) to promote brittle fracture propagation behaviour.

Research limitations/implications: The influence of coating thickness, pre-microcrack length, bone and artificial femoral stem elastic modulus on fracture behaviour is examined under different stress ratio using J-integral analysis approach.

Practical implications: The proposed finite element model can be easily accommodating different Hap coating thickness, pre-microcrack length, bone and artificial femoral stem elastic modulus to perform detailed parametric studies with minimal costly experimental works.

Originality/value: Limited research focussing on brittle fracture propagation behaviour of HAp coating in artificial femoral stem component. Thus, present study analysed the influence of coating thickness, pre-microcrack length, bone and artificial femoral stem elastic modulus on stress intensity factor (SIF) of HAp coating.

Keywords: Hydroxyapatite (HAp), Fracture, Stress intensity factor (SIF), Artificial femoral stem

Reference to this paper should be given in the following way:

C.H. Sheng, M. Nagentrau, N.H. Ibrahim, Prediction of brittle fracture propagation behaviour of hydroxyapatite (HAp) coating in artificial femoral stem component, Archives of Materials Science and Engineering 114/1 (2022) 34-41. DOI: https://doi.org/10.5604/01.3001.0015.9851

BIOMEDICAL AND DENTAL MATERIALS AND ENGINEERING

1. Introduction

Osteoarthritis is categorized as a debilitating disease that affects a great majority of elderly's [1,2]. The treatment for end-stage osteoarthritis is total joint arthroplasty, where surgery is performed to implant artificial structure to mimic the original function of the joint. The hip joint is one that is subjected to the most loads, thus, total hip arthroplasty is the most common joint arthroplasties [3-5]. Artificial hip modular stem which fixed into femur bone medullary cavity is made up of titanium alloys (Ti-6Al-4V). Ti-6Al-4V is low weight high strength material compared to other orthopaedic alloys [6,7]. In addition, Ti-6Al-4V alloy exhibiting good tissue tolerance, high wear and corrosion resistance. Cobalt-chrome alloy or stainless steel also used to fabricate modular stem but very seldom [8]. Uncemented artificial hip implants are one of two methods that achieves fixation of bone to Ti-6Al-4V implants through the use of bioactive materials such as hydroxyapatite that promotes bone ingrowth [9]. HAp is a brittle material and its application under fatigue loading condition doubts its survivability beyond ten years [10].

HAp displays ceramic-like properties which have high tensile strength but are often weaker against fatigue loading conditions. Leonakapul et al. [11] has revealed that the failure of hip implants often begins with cracks that propagates until the interface to initiate delamination. The HAp crack propagates from bone interface to Ti-6Al-4V interface then initiates delamination and cyclic loading promotes the delamination length [12-14]. As delamination reaches certain length, the interfacial strength between HAp and Ti-6Al-4V demoted and results in contact slip which can accelerate fretting wear behaviour [15]. These wear debris have shown to produce inflammatory responses when released into the body, inducing a life-threatening risk to the patients and leads to aseptic loosening of the hip implant.

The formation of HAp cracks is common due its ceramic nature which contains microcracks in its structure. Markovic et al. [16] found that the preparation method of sintering causes stress mismatch due to incomplete densification throughout the material causing the formation of cracks. Leonapakul et al. has revealed that simulated body fluid immersion reduces adhesive strength by up to 33% which changing compressive residual stress to tensile residual stress weakening interface strength and forming cracks [11]. Nimkherdpool et al. [17] concluded that coating dissimilar properties leads to residual stress which boosted by rapid cooling of quasi-melted splats creating a coat with varying phase composition and reduces crack formation resistance. Su et al. [18] has found that particle size of HAp used during preparation process influences crack formation where smaller initial particle size provides a smoother surface with significantly lesser cracks. In addition, Otsuka, et al. [13] has reported that crack propagation commences mainly at contact edge due to stress singularities.

Currently, far too little attention has been paid to brittle fracture propagation behaviour of HAp coating in artificial femoral stem component. Thus, present study is aimed to address the effect of coating thickness, pre-microcrack length, bone and artificial femoral stem elastic modulus on stress intensity factor (SIF) of HAp coating.

2. Methodology

2.1. Material

Ti-6Al-4V is the common material that widely used in artificial hip implants [19-21], meanwhile HAp coating is bio-ceramic material to promote bonding between bone and metallic implants [9]. Polyurethane (PU) Foam is assigned as contact pad to simulate human bone properties. The assigned material properties throughout the simulation are presented in Table 1.

Table 1.
FE simulation material properties data

No	Material	Young's modulus, E, GPa	Poisson's ratio, v
1.	PU foam (contact pad)	10	0.35
2.	HAp coating	70	0.24
3.	Ti-6Al-4V	110	0.33

2.2. Finite Element (FE) Model

The finite element contact configuration model shown in Figure 1 is a schematic view of a three-part model based on a fatigue experimental arrangement. The three parts consist of a Ti-6Al-4V implant substrate, HAp coating, and contact pad (bone), where a commercial FE software ABAQUS/Standard is employed throughout the static FE to predict the crack propagation behaviour HAp coating.

Two dimensional ¼ symmetric FE model is created to due to plane strain condition. The HAp coating is modelled with 10 mm length vertical pre-microcrack at the contact edge location to indicate stress singularity effect. The dimension of Ti-6Al-4V, HAp coating and PU foam (contact pad) are 4.0 mm x 2.0mm, 3.5 mm x 0.15 mm and 3.0 mm x 4.5 mm respectively. The pre-microcrack location in HAp coating is based on previous literature indicating crack formation as a result stress singularity [6]. Modelling a crack utilizes ABAQUS unique crack feature to define a crack

front and crack seam initially created with the partition feature as shown in Figure 2 to recognize the feature as a crack path with an opening.

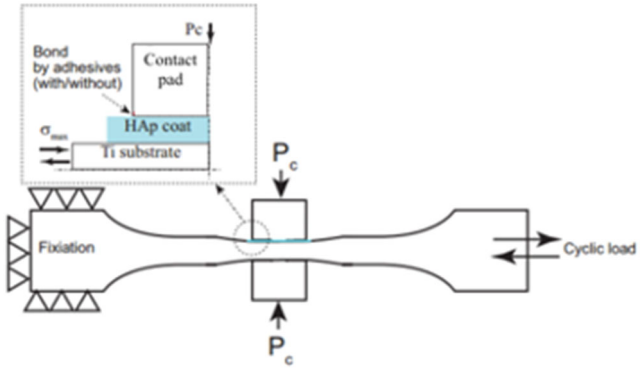

Fig. 1. Schematic view of contact configuration model

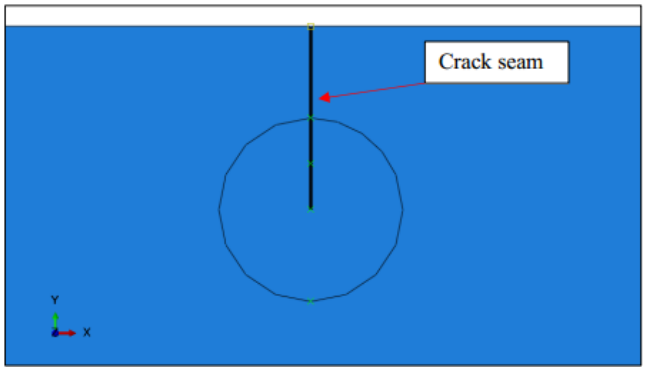

Fig. 2. Crack seam at pre-microcrack location

The complete assembly of FE model with loading and boundary condition is illustrated in Figure 3. The displacement and rotational movements of bottom and side regions are restricted in the y-axis and x-axis respectively. Additionally, tie constraints between contact pad-HAp and HAp-Ti-6Al-4V interfaces are introduced to assume perfect adhesion with little to no surface sliding. In both instances, the former is assigned as slave; the latter is assigned as master surface with Lagrange multiplier contact algorithm. The friction coefficient of 0.4 and 0.7 are set for contact pad-HAp and HAp-Ti-6Al-4V interfaces.

Figure 4a shows the finite element mesh module with linear quadrilateral plane strain elements. The appropriate mesh size of 10 µm at crack seam and 50 µm at contact region is assigned. Mesh transition from fine to coarse (from crack region to further region) is achieved via edge seeding technique. Mesh optimisation is attained via mesh transition to reduce computational time without affecting the result accuracy.

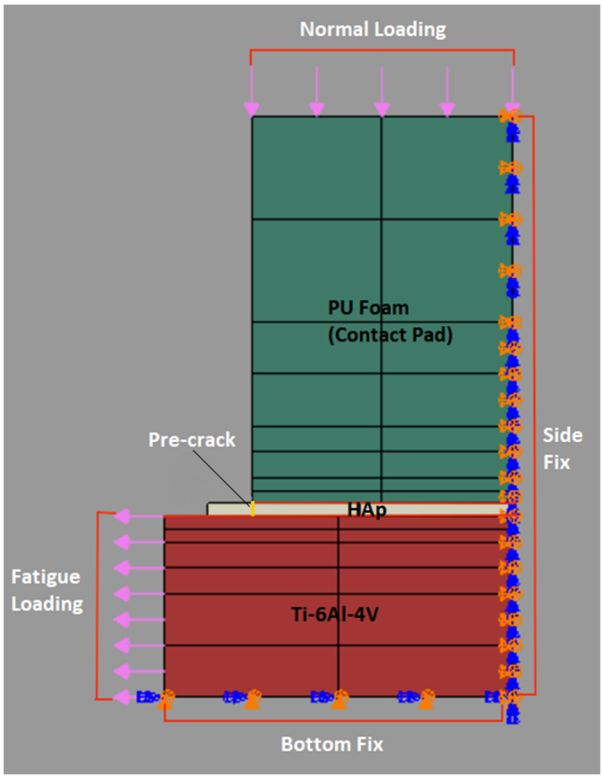

Fig. 3. FE model loading and boundary conditions

The simulation is executed in 3 static general steps with one second time period each such as normal loading (Step 1), maximum fatigue loading (Step 2) and minimum fatigue loading (Step 3) respectively. Normal loading of 20 MPa with maximum fatigue loading of 550 MPa and minimum fatigue loading of 55 MPa are assigned to represent artificial femoral stem component loading condition. Among the focussed variables of this study are HAp coating thickness (0.1-0.2 mm), pre-microcrack length (0.01-0.03 mm), bone elastic modulus (5-20 GPa) and hip implant modulus (110-250 GPa) under different stress ratio (R = 0.1, R = 10 and R = -1) condition. The variation in stress ratio is to represent artificial femoral stem subjected to tensile-tensile, compressive-compressive and tensile-compressive loading condition during various human activities. The result of FE simulation is extracted from ODB file as shown in Figure 4b. The result of stress intensity factor is extracted by setting history output (H-Output) request at the crack. The crack propagation is expected to occur when stress intensity factor (SIF) exceeds HAp material fracture toughness which is around 31.62 MPa/mm$^{1/2}$.

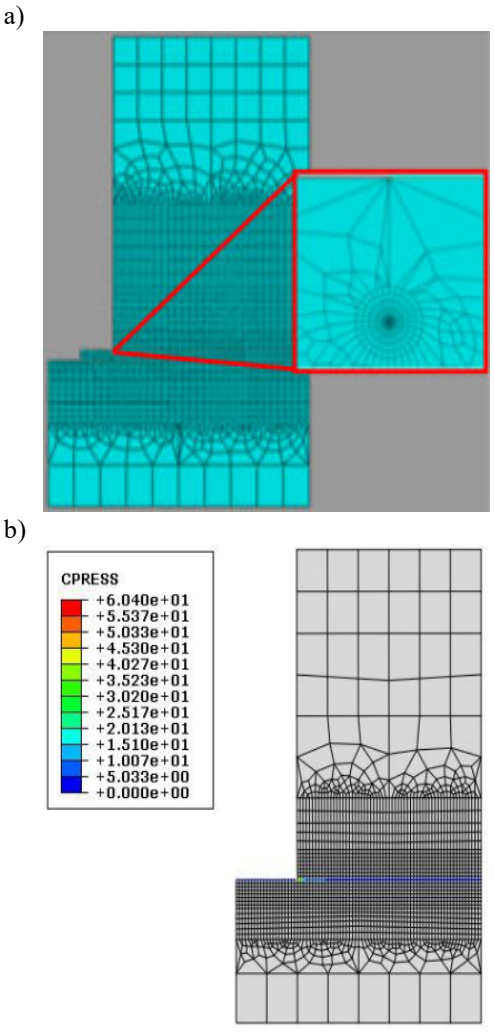

Fig. 4. (a) FE Mesh module and (b) FE simulation results

3. Results and discussion

3.1. The influence of coating thickness on SIF

Figure 5 shows the effect of coating thickness on the stress intensity factor affecting crack propagation. The results revealed that lower HAp coating thickness (0.1 mm) results in a significant stress intensity factor compared to higher coating thickness (0.2 mm) during maximum fatigue loading for all stress ratio condition. Stress intensity factor for all coating thickness for stress ratio R = 0.1 and R = -1 exceeds the fracture toughness of HAp to enable crack propagation due to tensile fatigue loading. Stress ratio, R = 10 exhibits insignificant stress intensity factor due to compressive fatigue loading which supress the crack propagation.

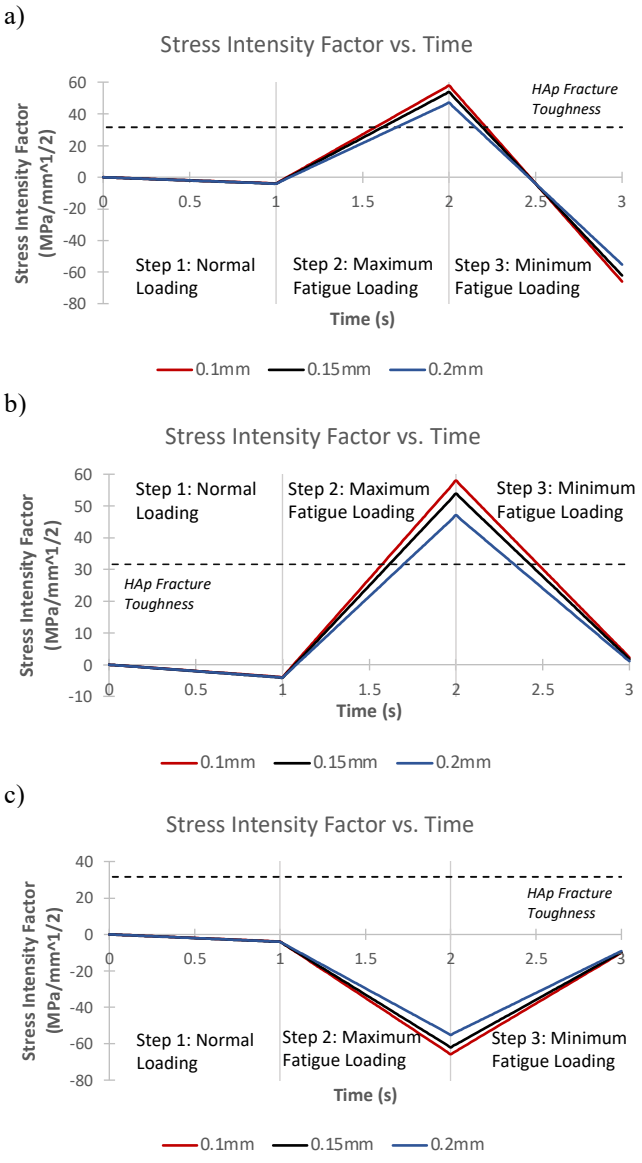

Fig. 5. Stress intensity factor (SIF) under different coating thickness: a) R = -1, b) R = 0.1, c) R = 10

3.2. The influence of pre-microcrack length on SIF

Figure 6 illustrates the effect of pre-microcrack length on stress intensity factor. The finding exhibits that lower pre-microcrack length (10 micron) results in a lower stress intensity factor compared to higher pre-microcrack length (30 micron). The stress intensity factor is significant during maximum fatigue loading compared to normal and minimum fatigue loading. The crack propagation is very obvious in tensile type fatigue loading (R = 0.1 and R = -1) compared to compressive fatigue loading.

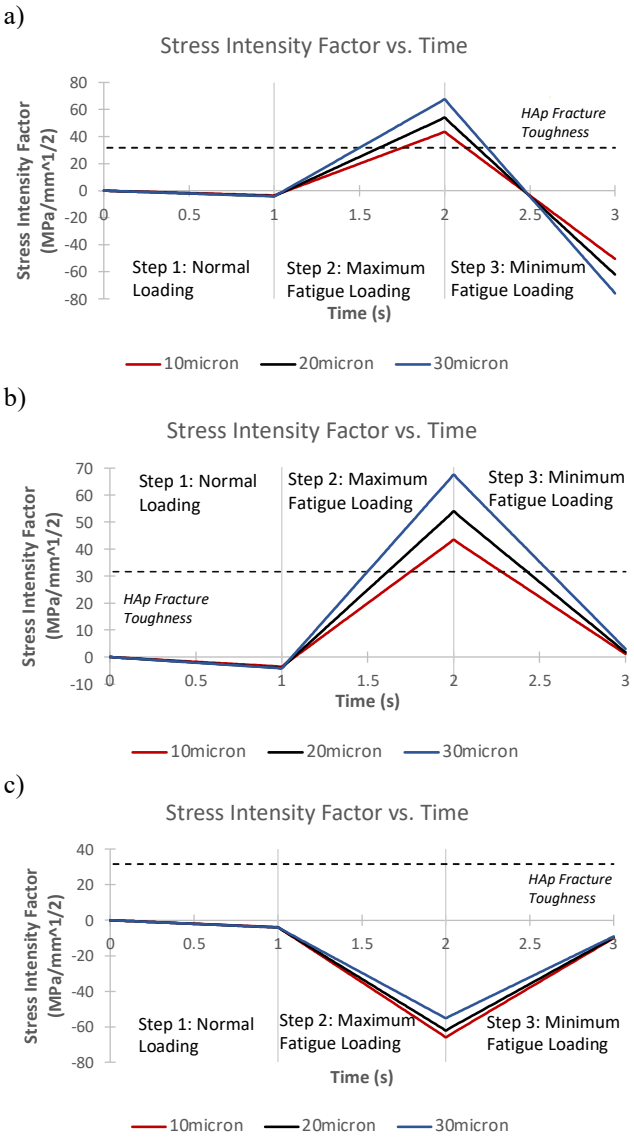

Fig. 6. Stress intensity factor (SIF) under different pre-microcrack length: a) R = -1, b) R = 0.1, c) R = 10

3.3. The influence of bone elastic modulus on SIF

Figure 7 displays the effect of bone elastic modulus on the stress intensity factor. The lower bone elastic modulus (5 GPa) records lower stress intensity factor compared to higher bone elastic modulus (20 GPa). Similar to previous cases, stress intensity factor is significant during maximum fatigue loading. Stress ratio R = 0.1 and R = -1 indicates clear trend of crack propagation as tensile fatigue loading accounts for higher stress intensity factor magnitude to exceed the fracture toughness of HAp coating.

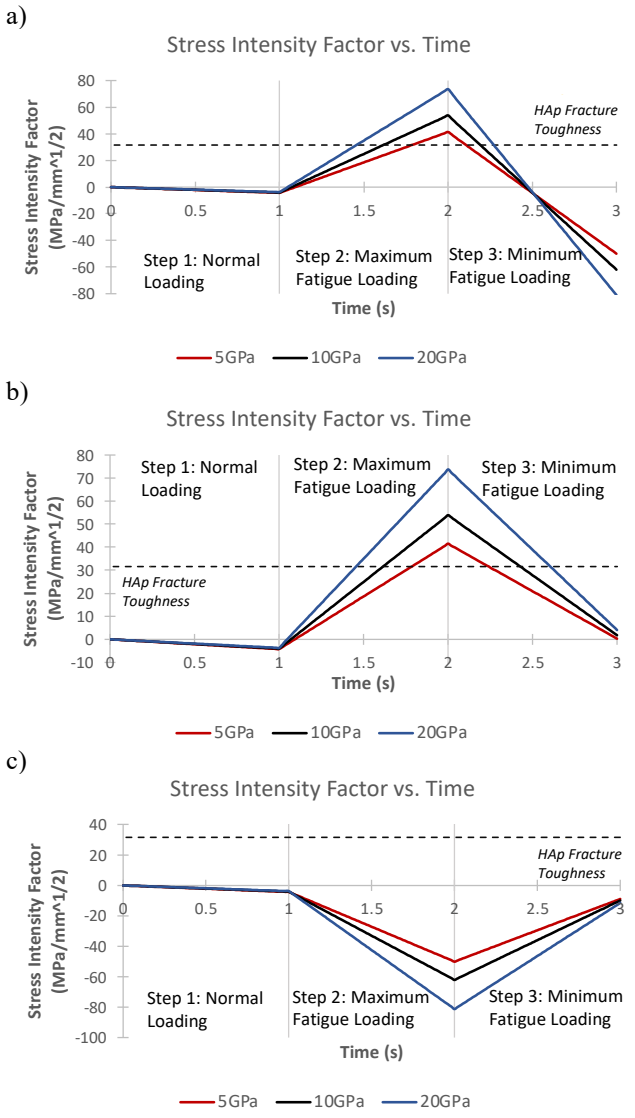

Fig. 7. Stress intensity factor (SIF) under different bone elastic modulus: a) R = -1, b) R = 0.1, c) R = 10

3.4. The influence of implant material on SIF

Figure 8 shows the effect of different hip implant materials (elastic modulus) on the stress intensity factor. Higher elastic modulus of hip implant material (250 GPa: cobalt chromium) results in a lower stress intensity factor compared to lower elastic modulus material (110 GPa: titanium). The peak stress intensity factor value for cobalt chromium is considerably lower than the HAp fracture toughness threshold. Whereas, titanium and stainless steel on the other hand with 110 GPa and 190 GPa elastic modulus indicates crack propagation.

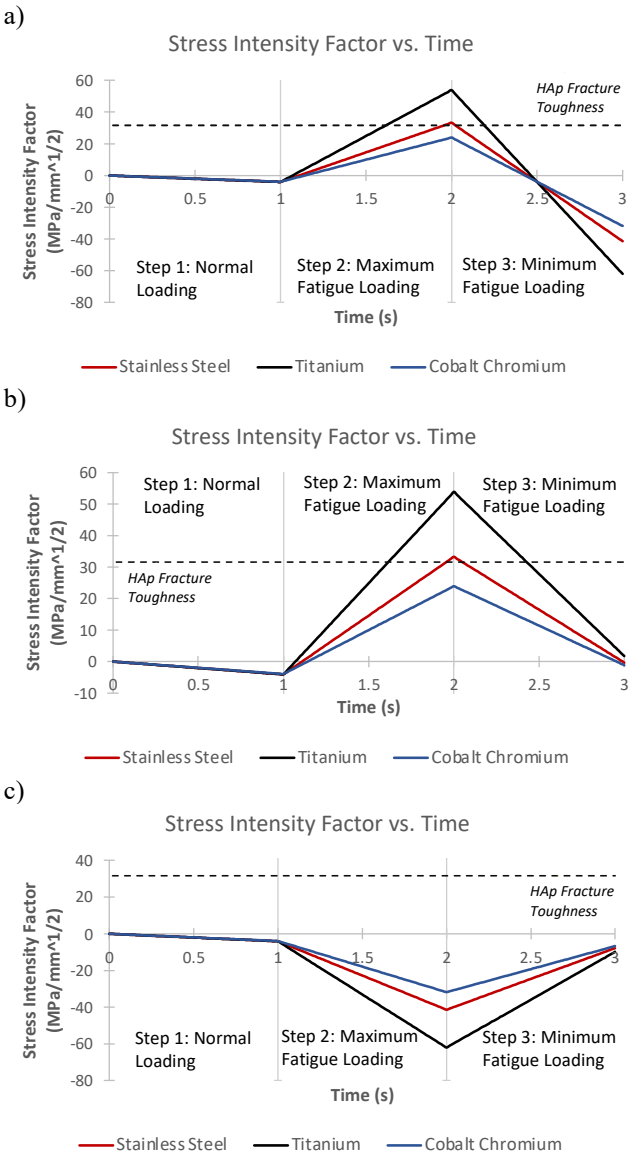

Fig. 8. Stress intensity factor (SIF) under different hip implant elastic modulus (material): a) R = -1, b) R = 0.1, c) R = 10

3.5. Discussion

Figure 9 illustrates peak stress intensity factor under different coating thickness, pre-microcrack length, bone elastic modulus and hip implant elastic modulus respectively. The result quite revealing that increasing coating thickness reduces stress intensity factor at the crack front region due to lower stress distribution in thicker coating [22-23]. Crack propagation is significant in tensile fatigue loading due to presence of contact slip and contact pressure.

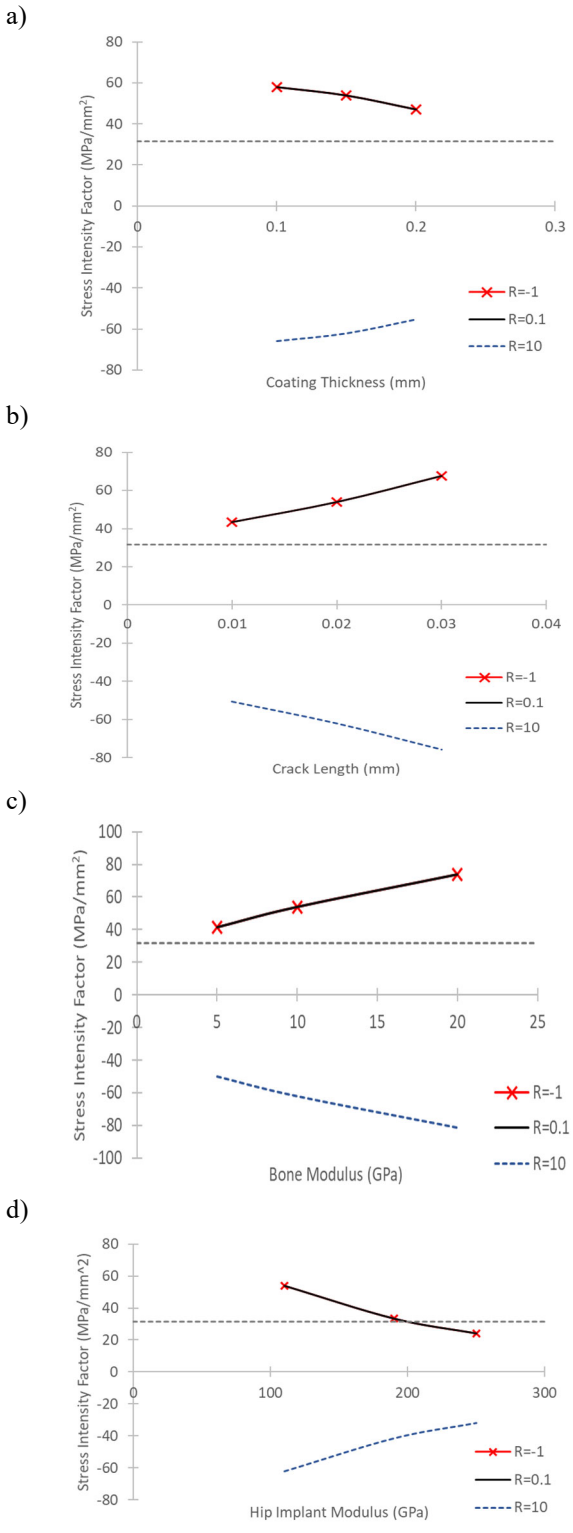

Fig. 9. Peak stress intensity factor under different (a) coating thickness (b) pre-microcrack length (c) bone elastic modulus and (d) hip implant elastic modulus

In addition, increasing pre-microcrack length records higher peak stress intensity factor at the crack front region. This finding is consistent with previous reported works which caused by opening of pre-microcrack.

Crack opening is mainly due to tangential displacement caused by maximum fatigue loading [22]. The peak stress intensity factor values are higher for increasing bone elastic modulus due to minimised elastic mismatch causing stress relaxation to promote contact slip which results in crack opening [5]. It is apparent that increasing hip implant elastic modulus recorded lower peak stress intensity factor due to more compliant coating on stiffer substrate. This enables the coating to absorb more energy and minimised crack propagation [23]. The reported results is consistent with previous researches done on crack propagation behaviour [24-27].

4. Conclusions

The predicted stress intensity factor (SIF) subjected to different HAp coating thickness, pre-microcrack length, bone elastic modulus and hip implant elastic modulus from FE analysis allows following conclusion to be drawn:

- Significant stress intensity factor is recorded for reduced coating thickness, pre-microcrack length and hip implant elastic modulus.
- Increased bone elastic modulus promotes stress intensity factor and brittle fracture propagation by exceeding HAp fracture toughness value.
- Brittle fracture propagation is significant in tensile type fatigue loading (R = 0.1 and R = -1) compared to compressive fatigue loading (R = 10).

Acknowledgements

This research work is supported by Japan Science and Technology Agency (JST), Ministry of Education Malaysia, Taylor's University Lakeside Campus, Universiti Tun Hussein Onn Malaysia, Nagaoka University of Technology, Japan and UOW Malaysia KDU University College.

Additional information

The article was presented at the 5th ICET 2021: 5th International Conference on Engineering Technology Virtual Conference KEMAMAN, Malaysia, October 25-26, 2021.

References

[1] C. Palazzo, C. Nguyen, M. M. Lefevre-Colau, F. Rannou, S. Poiraudeau, Risk factors and burden of osteoarthritis, Annals of Physical and Rehabilitation Medicine 59/3 (2016) 134-138. DOI: https://doi.org/10.1016/j.rehab.2016.01.006

[2] N. de l'Escalopier, P. Anract, D. Biau, Surgical treatments for osteoarthritis, Annals of Physical and Rehabilitation Medicine 59/3 (2016) 227-233. DOI: https://doi.org/10.1016/j.rehab.2016.04.003

[3] M.J. Lespasio, A.A. Sultan, N.S. Piuzzi, A. Khlopas, M.E. Husni, G.F. Muschler, M.A. Mont, Hip osteoarthritis: a primer, The Permanente Journal 22/1 (2018) 17-084. DOI: https://doi.org/10.7812/TPP/17-084

[4] K.D. Allen, Y.M. Golightly, Epidemiology of osteoarthritis: state of the evidence, Current Opinion in Rheumatology 27/3 (2015) 276-283. DOI: https://doi.org/10.1097/BOR.0000000000000161

[5] M. Nagentrau, A.M. Tobi, S. Jamian, Y. Otsuka, R. Hussin, Delamination-fretting wear failure evaluation at HAp-Ti-6Al–4V interface of uncemented artificial hip implant, Journal of the Mechanical Behavior of Biomedical Materials 122 (2021) 104657. DOI: https://doi.org/10.1016/j.jmbbm.2021.104657

[6] D. Apostu, O. Lucaciu, C. Berce, D. Lucaciu, D. Cosma, Current methods of preventing aseptic loosening and improving osseointegration of titanium implants in cementless total hip arthroplasty: a review, Journal of International Medical Research 46/6 (2018) 2104-2119. DOI: https://doi.org/10.1177/0300060517732697

[7] S.K. Fokter, A. Moličnik, R. Kavalar, P. Pelicon, R. Rudolf, N. Gubeljak, Why do some titanium-alloy total hip arthroplasty modular necks fail?, Journal of the Mechanical Behavior of Biomedical Materials 69 (2017) 107-114. DOI: https://doi.org/10.1016/j.jmbbm.2016.12.012

[8] M.A. Malahias, L. Kostretzis, A. Greenberg, V.S. Nikolaou, A. Atrey, P.K. Sculco, Highly porous titanium acetabular components in primary and revision total hip arthroplasty: a systematic review, The Journal of Arthroplasty 35/6 (2020) 1737-1749. DOI: https://doi.org/10.1016/j.arth.2020.01.052

[9] M. Nagentrau, A.L.M. Tobi, S. Jamian, Y. Otsuka, HAp Coated Hip Prosthesis Contact Pressure Prediction Using FEM Analysis, Materials Science Forum 991 (2020) 53-61. DOI: https://doi.org/10.4028/www.scientific.net/MSF.991.53

[10] M. Nagentrau, A.L.M. Tobi, S. Jamian, Y. Otsuka, Contact slip prediction in HAp coated artificial hip implant using finite element analysis, Mechanical Engineering Journal 6/3 (2019) 18-00562. DOI: https://doi.org/10.1299/mej.18-00562

[11] T. Laonapakul, A.R. Nimkerdphol, Y. Otsuka, Y. Mutoh, Failure behavior of plasma-sprayed HAp

coating on commercially pure titanium substrate in simulated body fluid (SBF) under bending load, Journal of the Mechanical Behavior of Biomedical Materials 15 (2012) 153-166. DOI: https://doi.org/10.1016/j.jmbbm.2012.05.017

[12] Y. Otsuka, D. Kojima, Y. Mutoh, Prediction of cyclic delamination lives of plasma-sprayed hydroxyapatite coating on Ti–6Al–4V substrates with considering wear and dissolutions, Journal of the Mechanical Behavior of Biomedical Materials 64 (2016) 113-124. DOI: https://doi.org/10.1016/j.jmbbm.2016.07.026

[13] Y. Otsuka, D. Kojima, Y. Miyashita, Y. Mutoh, Cyclic delamination life prediction model for plasma-sprayed hydroxyapatite coating on ti substrate under simulated body fluid, Materials Science and Engineering: C 67 (2016) 533-541. DOI: https://doi.org/10.1016/j.msec.2016.05.058

[14] Y. Otsuka, Y. Miyashita, Y. Mutoh, Effects of delamination on fretting wear behaviors of plasma-sprayed hydroxyapatite coating, Mechanical Engineering Journal 3/2 (2016) 15-00573. DOI: https://doi.org/10.1299/mej.15-00573

[15] F. Liu, Micro-CT and Micro-FE analysis of stress transfer of femoral stems, PhD Thesis, Ludwig Maximilian University of Munich, Munich, 2021.

[16] S. Marković, M.J. Lukić, S.D. Škapin, B. Stojanović, D. Uskoković, Designing, fabrication and characterization of nanostructured functionally graded HAp/BCP ceramics, Ceramics International 41/2/B (2015) 2654-2667. DOI: https://doi.org/10.1016/j.ceramint.2014.10.079

[17] A.R. Nimkerdphol, Y. Otsuka, Y. Mutoh, Effect of dissolution/precipitation on the residual stress redistribution of plasma-sprayed hydroxyapatite coating on titanium substrate in simulated body fluid (SBF), Journal of the Mechanical Behavior of Biomedical Materials 36 (2014) 98-108. DOI: https://doi.org/10.1016/j.jmbbm.2014.04.007

[18] Y. Su, K. Li, L. Zhang, C. Wang, Y. Zhang, Effect of the hydroxyapatite particle size on the properties of sprayed coating, Surface and Coatings Technology 352 (2018) 619-626. DOI: https://doi.org/10.1016/j.surfcoat.2018.08.052

[19] W.A. Siswanto, M. Nagentrau, A.M. Tobi, M.N. Tamin, Prediction of plastic deformation under contact condition by quasi-static and dynamic simulations using explicit finite element analysis, Journal of Mechanical Science and Technology 30/11 (2016) 5093-5101. DOI: https://doi.org/10.1007/s12206-016-1027-3

[20] M. Nagentrau, W.A. Siswanto, M. Tobi, A. Latif, Predicting the sliding amplitude of plastic deformation in the reciprocating sliding contact, ARPN Journal of Engineering and Applied Sciences 11/4 (2016) 2266-2271.

[21] W.A. Siswanto, M. Nagentrau, M. Tobi, A. Latif, Prediction of residual stress using explicit finite element method, Journal of Mechanical Engineering and Sciences 9 (2015) 1556-1570. DOI: http://dx.doi.org/10.15282/jmes.9.2015.3.0151

[22] M.L. Mohsin, A.L.M. Tobi, W.A. Siswanto, M. N. Tamin, Finite element analysis of stress intensity factor of pre-cracked coated substrate under contact sliding, Proceedings of the 36th International Electronics Manufacturing Technology Conference, Johor, Malaysia, 2014, 1-4. DOI: https://doi.org/10.1109/IEMT.2014.7123099

[23] A.M. Tobi, P.H. Shipway, S.B. Leen, Finite element modelling of brittle fracture of thick coatings under normal and tangential loading, Tribology International 58 (2013) 29-39. DOI: https://doi.org/10.1016/j.triboint.2012.08.024

[24] R.A. Mahdavinejad, Prediction of cannon barrel life, Journal of Achievements in Materials and Manufacturing Engineering 30/1 (2008) 11-18.

[25] M. Szutkowska, M. Boniecki, Crack growth resistance of Al_2O_3-ZrO_2 (nano)(12 mol% CeO_2) ceramics, Journal of Achievements in Materials and Manufacturing Engineering 22/1 (2007) 41-44.

[26] D. Kwiatkowski, J. Nabiałek, P. Postawa, Influence of injection moulding parameters on resistance for cracking on example of PP, Journal of Achievements in Materials and Manufacturing Engineering 17/1-2 (2006) 97-100.

[27] T.M. Lenkovskiy, V.V. Kulyk, Z.A. Duriagina, L. V. Dzyubyk, V.V. Vira, A.R. Dzyubyk, T.L. Tepla, Finite elements analysis of the side grooved I-beam specimen for mode II fatigue crack growth rates determination, Journal of Achievements in Materials and Manufacturing Engineering 86/2 (2018) 70-77. DOI: https://doi.org/10.5604/01.3001.0011.8238